ELSEVIER

Journal of Fluids and Structures 22 (2006) 941–947

JOURNAL OF FLUIDS AND STRUCTURES

www.elsevier.com/locate/jfs

Empirical scaling of antisymmetric stratified wakes

S. Gallet[a], P. Meunier[b,*], G.R. Spedding[a]

[a]*Department of Aerospace & Mechanical Engineering, University of Southern California, Los Angeles, CA, USA*
[b]*Institut de Recherche sur les Phénoménes Hors Equilibre, 49, av. Joliot-Curie, F-13384 Marseille, France*

Received 4 October 2005; accepted 14 April 2006
Available online 25 July 2006

Abstract

Initially turbulent wakes of a propelled cylinder at nonzero angles of yaw to the mean flow were measured in the horizontal centerplane plane up to approximately 100 buoyancy times, where vertical velocities are very small. The profiles of mean velocity were found to be antisymmetric throughout their lifetime, with both width and maximum velocity decaying at the same rate as previously studied momentum wakes. The maximum velocity of the profile is proportional to the angle of yaw, but the width is constant. Both the mean flow and fluctuating quantities show that the late wake is self-similar, with scaling laws that are consistent with previous work on propelled and drag wakes.

1. Introduction

In a homogeneous fluid, the late stages of a turbulent bluff-body wake can be described by the theory of a self-preserved wake [see Tennekes and Lumley (1972)]. However, the presence of even a weak stable stratification can significantly modify this picture, imposing an anisotropy that must be accounted for and bringing internal wave motions into the dynamics. This is the case of the wakes of submarines and of mountains or islands, for which the ocean and the atmosphere are stably stratified.

Lin and Pao (1979) showed that the stratification diminishes the vertical velocities and thus prevents the growth of the wake in the vertical direction after a time $Nt \approx 2$ (N is the Brünt Vaisala frequency, $N^2 = (g/\rho_0)(\partial\rho/\partial z)$, where z is the vertical direction, ρ is the density and g is the gravitational acceleration), leading to coherent vortices that are small in the vertical compared with the horizontal direction. Since horizontal growth rates do not increase commensurately, the defect velocity decays more slowly, and can be as high as 10 times larger than in the absence of stratification. Spedding (1997) showed that this stage lasts up to $Nt \approx 50-100$, and that the defect velocity then decays again with the same exponent as in a homogeneous fluid. Most of the late-wake measurements have been obtained for spheres [e.g., Chomaz et al. (1993), Spedding et al. (1996), Spedding (1997)]. The effect of the shape of the bluff body was investigated by Meunier and Spedding (2004), who showed that all bluff-body wakes, regardless of body geometry, could be rescaled with parameters that depended only on the initial momentum flux in the wake. Meunier and Spedding (2006) described the wakes of propelled bodies, finding similarly general scaling behavior for all but a small class of wakes that were almost exactly momentumless. Furthermore, if the wakes were at this (almost singular) point, a third class of antisymmetric velocity profile was found behind a body having a small angle of yaw. This paper presents systematic and

*Corresponding author.
E-mail address: meunier@irphe.univ-mrs.fr (P. Meunier).

0889-9746/$ - see front matter
doi:10.1016/j.jfluidstructs.2006.04.017

quantitative experimental results of such wakes behind a propelled cylinder at small angle of yaw. The important parameters will be defined and quantified. Decay rates of velocity, turbulent Reynolds number and kinetic energy will be compared with the existing values in the literature.

2. Procedure

2.1. Experimental set-up

A cylinder of diameter $D = 2.7\,\text{cm}$ and length $L = 15.6\,\text{cm}$ is towed through a $2.4 \times 2.4\,\text{m}$ water tank filled to a height $H = 22\,\text{cm}$, as described in detail in Spedding et al. (1996). The tank is filled using the standard two-tank method, mixing between fresh water ($\rho_f = 1.0\,\text{kg/m}^3$) and salt water ($\rho_s = 1.1\,\text{kg/m}^3$), to yield a linear vertical density gradient so that $N = 1.8\,\text{rad/s}$; ρ_f and ρ_s are selected so polystyrene beads of diameter $d = 1\,\text{mm}$ and density $\rho = 1.04965 \pm 0.00005\,\text{kg/m}^3$ rest on an isopycnal at the horizontal centerline of the cylinder. The beads are illuminated using four 500 W floodlights, and a custom digital particle imaging velocimetry method (DPIV) (Fincham and Spedding, 1997) is used to determine velocity fields u, v in the x, y horizontal plane, together with their spatial gradients.

In order to accurately control the yaw angle, and in contrast to previous mounting methods, the cylinder is mounted on a streamlined carriage via a hollow sting (3 mm in diameter). A tight friction fit and set-screw to the carriage post provide convenient submergence and removal of the body, and allow yaw angles to be reliably and precisely set. The propulsion system inside the body consists of a small DC motor powered by a 4.8 V battery through a 4 channel 75 MHz FM RC transmitter and GWS ICS50 micro speed-control.

In the laboratory frame of reference, shown in Fig. 1, the body is towed steadily along the x-axis with speed U_b. An experiment consists of one towing of the body through the length of the tank, and digital image acquisition using a Pulnix TM9701 CCD camera mounted above the tank until $Nt = 300$, with $t = 0$ defined when the body center crosses the center of the $84 \times 61\,\text{cm}$ capture window. The propeller is started just before the body is towed and takes less than 0.5 s to reach the set angular velocity. It is shut off by the transmitter approximately 1–2 cm before the body comes to rest, to prevent a jet from impinging upon the wake at late times. Since the resolution of towing speed is higher than that of the propulsion system, the propeller angular velocity is held constant and experiments are conducted by systematically varying the tow speed until the measured momentum flux in the wake is zero. Once this momentumless speed, denoted U_c is known, experiments are repeated with $\alpha = 2^\circ, 3^\circ, 5^\circ$.

2.2. Flow definitions

Two nondimensional parameters are used to classify flows in a stratified medium: the Reynolds number $\text{Re} \equiv U_b D/\nu$, where ν is the kinematic viscosity, and a Froude number based on cross-section radius, $\text{F} \equiv 2U_b/ND$. Experiments were conducted for $\text{Re} = 6600$, $\text{F} = 10$, for which the inner wake is fully turbulent, and the late-wake centerline flowfield is not affected by the tank boundaries.

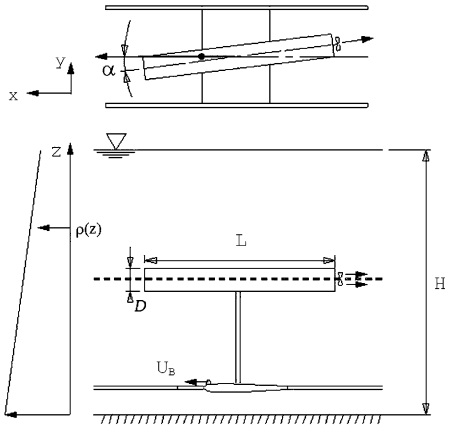

Fig. 1. Top and side views of the carriage and propelled cylinder. The black dotted line at the body centerline represents the bead sheet.

Because the inner wake is turbulent, the flow can be split into nonzero mean and fluctuating parts, $(u, v) = (U, V) + (u', v')$. Mean profiles plotted for each Nt value are obtained by averaging the u velocity components of one image along the x-axis (direction of travel) and are denoted $\langle u \rangle$. In these experiments, this is equivalent to a time average over $Nt = 6$, which is small compared to the total time span of the experiment. Consistent offsets in the profile tails (typically $u_{\text{off}} \leqslant 10\%$ of the peak defect magnitude) were removed by assuming that all averaged horizontal velocity components should be zero far ($y > 15D$), from the wake centerline. These offsets were mainly due to slow back and forth motion of the entire fluid in the tank caused by reflected internal waves. Apart from mean profiles, the cross-fluctuations, $\langle u'v' \rangle$ and the quadratic fluctuations $\langle u'^2 + v'^2 \rangle^{1/2}$ of velocity are used to compare this flow with self-preserved wakes found in the literature. It is useful to define the momentum thickness $D_{\text{mom}} = \text{D}\sqrt{(c_{\text{d}}/2)}$ of the bluff body and its corresponding Froude number $\text{F}_{\text{mom}} \equiv 2\,U_b/ND_{\text{mom}}$ in order to compare these results with the universal laws found in stratified momentum wakes (Meunier and Spedding 2004).

3. Results

3.1. Flow structure

Experimentally, three regimes have been distinguished behind propelled bodies in stratified flows depending on the ratio of tow-speed to the true self-propelled speed. These are shown in Fig. 2 in the form of instantaneous vertical vorticity fields (the body was towed from right to left). The first regime, called the momentum-regime and shown in Fig. 2(a), reveals two layers of opposite-signed vortices, which is equivalent to a mean Gaussian profile of velocity in the wake. Here the tow speed is slightly greater than U_c, creating a net positive mean flow in the wake on the order of 7% of U_c. Meunier and Spedding (2006) successfully re-scaled flow parameters of towed propelled bodies with those of simply towed bodies based on the difference between the tow speed and the momentumless speed U_c, for which the net momentum in the wake would be zero. Wakes of propelled bodies under such conditions are classified as within the momentum-regime.

The second regime, truly momentumless, cannot be re-scaled in the same fashion, as the tow speed is exactly equal to U_c. Attempts to quantify this flow regime in a general way have failed as there appears to be no organizing structure. This can be seen in Fig. 2(b), where opposite-signed vortices lie within a band, but with no apparent order.

The third regime is also momentumless, but involves a slight asymmetry of the body. This regime was discovered when the propelled body had a small angle of yaw. Fig. 2(c) shows the qualitatively different nature of this regime from the previous case with zero angle of yaw. The wake is composed of three layers of alternating opposed-sign vortices, whose pattern reverses for opposite angles of yaw. The organized layers lead to quantifiable mean profiles and fluctuating quantities.

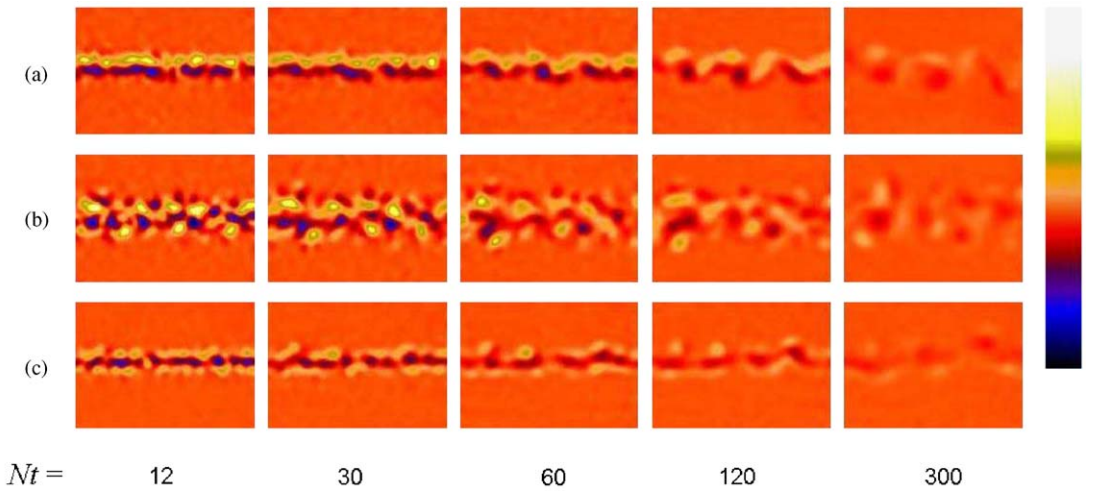

Fig. 2. Vertical in-plane vorticity ω_z revealing three wake structures for towed-propelled bodies: in (a) when the towing speed is different from the momentumless speed, in (b) when they are exactly equal, and in (c) for the same conditions as (b) but with a small angle of yaw. The color bar extremes are scaled at $0.02, 0.04$ and $0.02U_b/D$, respectively.

3.2. Mean flow

Using the Reynolds decomposition defined in Section 2.2, mean profiles can be plotted, for $4<Nt<300$, and are shown in Fig. 3. As can be seen in Fig. 3(a), these mean profiles are antisymmetric, and remain so throughout the measurable lifetime of the wake. This is in contrast to profiles of wakes in the momentum-regime, which can be described by Gaussian distributions. For propelled bodies at an angle of yaw, the resultant wake can be pictured as a linear combination of a drag wake with mean negative velocity and a thrust jet of mean positive velocity. As shown in Fig. 3(b), for increasing angles the negative peak (due to the drag) increases, and while the total momentum in the wake is zero for $\alpha = 2^0$, there is a small net momentum at $\alpha = 5^0$. The tow speed was not increased for each angle, even though it would correct for the increase in drag, because it would substantially increase the number of runs to yield one usable experiment. For increasing α, as shown in Fig. 3(b), the defect amplitude also increases though the direct correspondence to α is difficult to ascertain.

The profiles of $\langle U\rangle/U_b$ can be described as odd functions of y/D, whose maximum amplitude is $U_1 = \max(\langle U\rangle) - \min(\langle U\rangle)$ and inner wake width is $L_1 = y_{\max} - y_{\min}$, where $y_{\max}$ is the y/D position of the maximum value of the profile and $y_{\min}$ the position of the minimum.

The evolution of U_1 and L_1 as a function of Nt are plotted in Fig. 4, re-scaled with F to be comparable with previous data in the literature. The re-scaling is needed in the momentum-regime to collapse data with varying F. In Fig. 4(a),

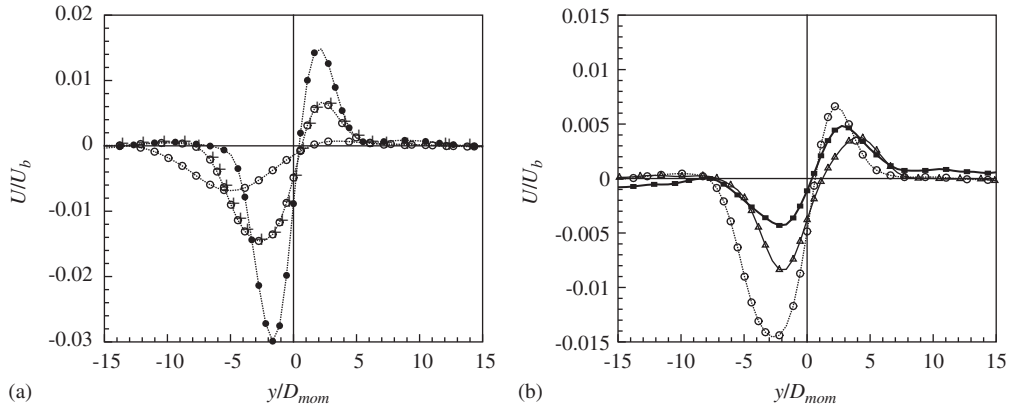

Fig. 3. Profiles of mean velocity. (a) For $\alpha = 5^\circ$: •, at $Nt = 20$; ⊕, $Nt = 100$; ○, $Nt = 300$. (b) At $Nt = 100$: ■, $\alpha = 2^\circ$; △, $\alpha = 3^\circ$; ○, $\alpha = 5^\circ$.

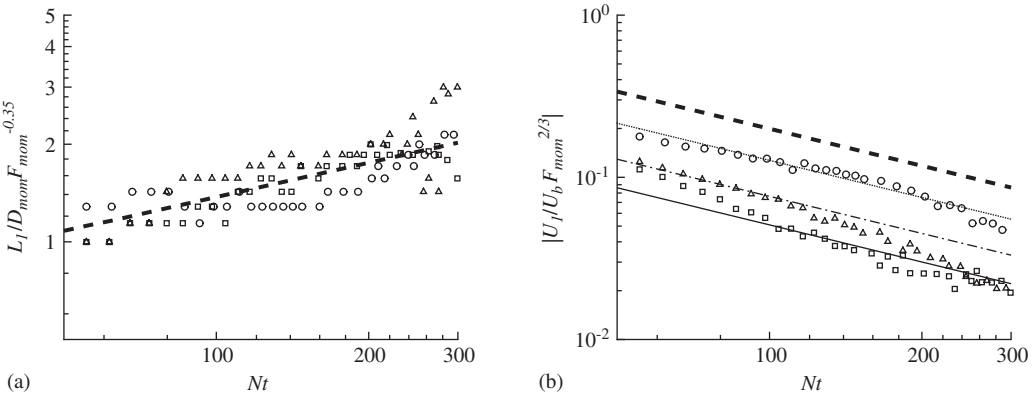

Fig. 4. (a) Wake width and (b) maximum amplitude of the mean velocity profiles for yaw angles $\alpha = 2^\circ(\square), 3^\circ(\triangle), 5^\circ(\circ)$. The thick dashed line represents Eq. (1) in (a) and Eq. (2) in (b) with $C = 6.6$. In (b) Eq. (2) is plotted with $C = \alpha \cdot (0.0055 \pm 0.0005)$: —, $\alpha = 2^\circ$; $-\cdot-$, $\alpha = 3^\circ$; …, $\alpha = 5^\circ$.

L_1 is seen to grow with Nt at a rate similar to the universal decay law for momentum wakes, defined as

$$\frac{L_1}{D_{\text{mom}}}\mathrm{F}^{-0.35} = 0.275(Nt)^{0.35}, \tag{1}$$

where $D_{\text{mom}} = D\sqrt{c_d/2}$ and plotted as a thick dashed line. c_d is the drag coefficient for the body with no stratification and can be looked up in reference texts; its use is appropriate at moderate to high F when the drag determined by the near wake is not strongly influenced by stratification. Here L_1 agrees well with the momentum case (the discrete jumps in L_1 are caused by the finite resolution of the original gridded data, which have not been further interpolated), and no dependence on angle is apparent, which is reasonable at least for small angles.

U_1 however, plotted in Fig. 4(b), shows a clear dependence on α. The decay law for the momentum-regime is shown with a thick dashed line, defined by

$$\frac{U_1}{U_B}\mathrm{F}^{2/3} = C(Nt)^{-0.76} \tag{2}$$

with $C = 6.6$. In the asymmetric regime, this simple model also predicts U_1 if we take $C(\alpha) = \alpha(0.0055 \pm 0.0005)$. This relationship is plotted in Fig. 4(b) for $\alpha = 2^\circ, 3^\circ, 5^\circ$, and agrees quite well with the experimental data in the sense that the *ad hoc* magnitude correction appears good and there are no systematic deviations from the straight lines over the three angles considered. Direct proportionality apparently occurs at small angles, but obviously breaks down theoretically at $\alpha = \pi/2$, and most probably earlier in experiments due to a more complex 3-D flow structure.

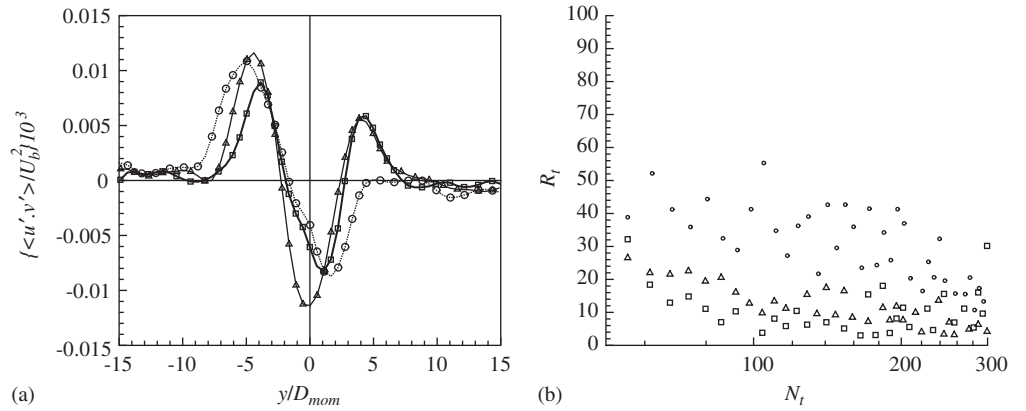

Fig. 5. (a) Profiles of cross-fluctuation velocity for yaw angles $\alpha = 2^\circ(\square), 3^\circ(\triangle), 5^\circ(\circ)$ at $Nt = 100$. (b) The turbulent Reynolds number defined in Eq. (4).

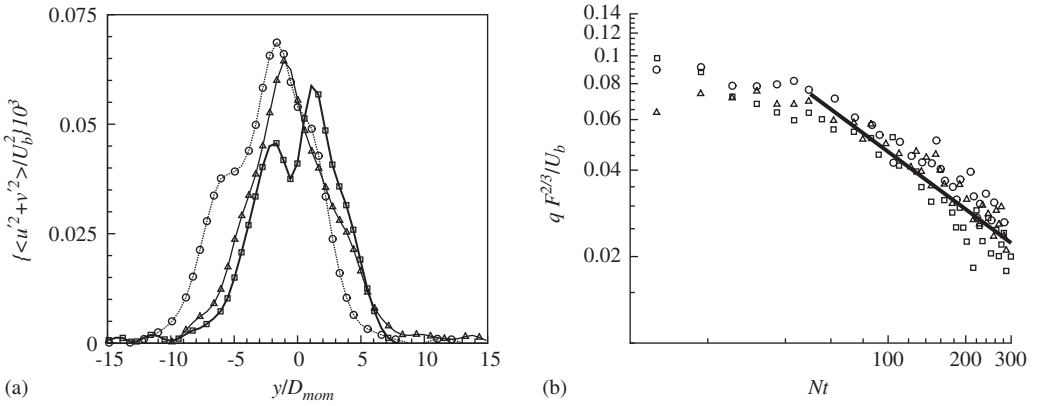

Fig. 6. (a) Mean profiles of turbulent kinetic energy and (b) its re-scaled peak value for yaw angles $\alpha = 2^\circ(\square), 3^\circ(\triangle), 5^\circ(\circ)$, compared to an $Nt^{-2/3}$ power-law decay rate (solid line).

3.3. Fluctuating quantities

In a turbulent flow, the cross-fluctuations of velocity can be related to the mean shear by

$$\langle u'v' \rangle = \nu_T \frac{\partial U}{\partial y}, \tag{3}$$

where ν_T is the turbulent eddy viscosity. The cross-fluctuation profiles are plotted in Fig. 5(a), and do seem proportional to the derivative of the mean profiles plotted in Fig. 3(b). The three peaks of fluctuations align with the three areas of maximum slope of the mean profile, and the signs are consistent. This supports the idea that the antisymmetric wake is also self-preserved, and diffuses by the action of the cross-fluctuations of velocity $\langle u'v' \rangle$, themselves driven by the mean shear $\partial U/\partial y$. This regime, just as the drag or momentum-regimes, may therefore be described under the assumption of a constant eddy viscosity ν_T. One can define a turbulent Reynolds number relating the mean flow magnitude to the cross-fluctuations magnitude,

$$R_t = \frac{|U_1|L_1}{\nu_T} = \frac{U_1^2}{\langle u'v' \rangle_{\max}}, \tag{4}$$

which in turn provides a check for the constant eddy-viscosity assumption. The results in Fig. 5(b), show R_t to be at best weakly dependent on α, though the values are scattered. Overall a constant R_t approximation is reasonable for the full range, and very good after $Nt = 100$. A mean value of the turbulent Reynolds number for $\alpha \leqslant 5^\circ$ lies around $R_t = 25 \pm 20$. For nonpropelled body experiments, Meunier and Spedding (2004) found a similar value of $R_t \simeq 15$, and concurred that it may not be considered constant until after $Nt = 100$.

As noted in Spedding et al. (1996) for the case of a towed sphere, the turbulent kinetic energy in the inner wake $q = \langle u'^2 + v'^2 \rangle_{\max}^{1/2}$, can be expected to scale as

$$\frac{q}{U_b} \mathrm{F}^{2/3} \sim (Nt)^{-2/3} \tag{5}$$

for self-similar evolution. The averaged profiles of quadratic fluctuations are plotted in Fig. 6(a). They are wedge-shaped, with a single peak in the center of the wake. The peak value can be used to compare the decay of the turbulent kinetic energy with the expected power-law decay rate for a self-preserved wake. Both parts of Eq. (5) are plotted in Fig. 6(b), and agree well for $Nt \geqslant 80$.

4. Discussion and conclusions

The wakes of propelled bodies in stratified fluids have previously been quantified both in the momentum and momentumless regimes, for axisymmetric conditions and now with an angle of yaw. At nonzero angles of yaw, the wakes are simpler to predict than for $\alpha = 0$.

The mean velocity profile is antisymmetric and decays stably. It can be described fully by L_1 and U_1 as a function of α. Both the cross-fluctuations of velocity and the kinetic energy show that some theory of self-preserved wakes is applicable, at least for $Nt \geqslant 100$. Since the antisymmetric profile can contain some momentum, the transition from a Gaussian momentum wake to an asymmetric zero-momentum wake is smooth, unlike for $\alpha = 0$ as shown by Meunier and Spedding (2006), though the asymmetric profile is quickly overtaken by the drag away from the zero-momentum point.

This work provides further evidence that wakes of submerged bodies will almost always be different from those discovered for the exactly momentumless case. It is rare that a body will travel at exactly zero degrees angle of attack, unless the specified route is exactly aligned with the mean flow, or unless the mean flow is negligible (and uniform, and steady). Moreover, almost any navigation or turning manoeuvre will put the flow into the small yaw angle regime described here. Thus, the family of robust scaling relationships for initially turbulent bluff-body wakes is expanded by those found in the small yaw angle regime, and they can be considered applicable to most practical situations.

Acknowledgment

The support of ONR Grant no. N00014-04-1-0034 administered by Dr R. Joslin is most gratefully acknowledged.

References

Chomaz, J.M., Bonneton, P., Hopfinger, E.J., 1993. The structure of the near wake of a sphere moving horizontally in a stratified fluid. Journal of Fluid Mechanics 254, 1–21.

Fincham, A.M., Spedding, G.R., 1997. Low-cost high-resolution dpiv for turbulent flows. Experiments in Fluids 23, 449–462.

Lin, J.T., Pao, Y.H., 1979. Wakes in stratified fluids: a review. Annual Review of Fluid Mechanics 11, 317–338.

Meunier, P., Spedding, G.R., 2004. A loss of memory in stratified momentum wakes. Physics of Fluids 16 (2), 298–305.

Meunier, P., Spedding, G.R., 2006. Stratified propelled wakes. Journal of Fluid Mechanics 552, 229–256.

Spedding, G.R., 1997. The evolution of initially turbulent bluff-body wakes at high internal froude number. Journal of Fluid Mechanics 337, 283–301.

Spedding, G.R., Browand, F.K., Fincham, A.M., 1996. Turbulence, similarity scaling and vortex geometry in the wake of a towed sphere in a stably stratified fluid. Journal of Fluid Mechanics 314, 53–103.

Tennekes, H., Lumley, J.L., 1972. A First Course in Turbulence. M.I.T. Press, Cambridge, MA.